

## Fast EXAFS in synchronous scanning mode at PETRA P06

This content has been downloaded from IOPscience. Please scroll down to see the full text.

2016 J. Phys.: Conf. Ser. 712 012020

(<http://iopscience.iop.org/1742-6596/712/1/012020>)

View [the table of contents for this issue](#), or go to the [journal homepage](#) for more

Download details:

IP Address: 131.169.95.181

This content was downloaded on 14/06/2016 at 11:51

Please note that [terms and conditions apply](#).

## Fast EXAFS in synchronous scanning mode at PETRA P06

Roman Chernikov<sup>1</sup>, Edmund Welter<sup>1</sup>, Wolfgang Caliebe<sup>1</sup>, Gerd Wellenreuther<sup>2</sup>  
and Gerald Falkenberg<sup>1</sup>

<sup>1</sup> DESY Photon Science, Notkestrasse 85, 22607 Hamburg, Germany

<sup>2</sup> European XFEL, Albert-Einstein-Ring 19, 22607 Hamburg, Germany

E-mail: roman.chernikov@desy.de

**Abstract.** First fast EXAFS spectra have been successfully measured at the Hard X-ray Micro-probe Beamline P06 (PETRA III) synchronously scanning the U32 undulator gap and the monochromator Bragg axis. Stability and spatial homogeneity of the beam are proved to be the limiting factors for the quality of the EXAFS spectra, whereas the performance of the data acquisition electronics limits the energy resolution when total scan time is reduced to 30 seconds. Results of the test measurements give us the estimate of the utmost performance of 5-10 seconds per full EXAFS scan considering certain hardware modifications.

### 1. Introduction

One of the goals in an EXAFS experiment is to measure the highest quality spectra in the shortest time; in practice a typical measurement at a bending magnet source could last up to 20-30 minutes in order to accumulate decent signal-to-noise level. Nowadays the flux created by insertion devices is high enough to provide sufficient photon counts even at millisecond timescales. The efficiency of conventional step scans therefore tends to zero, as a significant portion of the time is wasted for monochromator movement and stabilization. Moreover long exposure of the samples to high intensity beam raises the problem of radiation damage. The general solution in this case is operation in continuous mode, when the energy is scanned non-stop at fixed velocity and the signal is read out on the fly. This approach works flawlessly at bending magnets or wigglers that generate a smooth spectrum, however its implementation at an undulator source is non-trivial – one must either scan the undulator gap together with the Bragg angle [1,2] or taper the undulator gap [3,4]. The former guarantees higher flux and predictable spatial profile of the beam for the price of lower mechanical reliability and the need for precise monochromator-undulator movement synchronization. The latter suffers from the limited energy bandwidth and complicated spatial structure of the beam changing along the scan. Both approaches are feasible at the Hard X-Ray Micro-probe Beamline P06 (PETRA III). Here we present the results of our attempts to apply the synchronous scanning for the fast EXAFS measurement on powder samples.

### 2. Synchronization of the undulator and monochromator movement

Details of the beamline layout are published elsewhere [5], the most important are the PETRA III spectroscopy undulator U32 ( $\lambda_u=31.4\text{mm}$ ) and the FMB-Oxford High Heatload Monochromator. All beamline components including the measurement system are controlled via TANGO, the measurement routine was written in Python invoking the pyTango module according to the flowchart at figure 1.



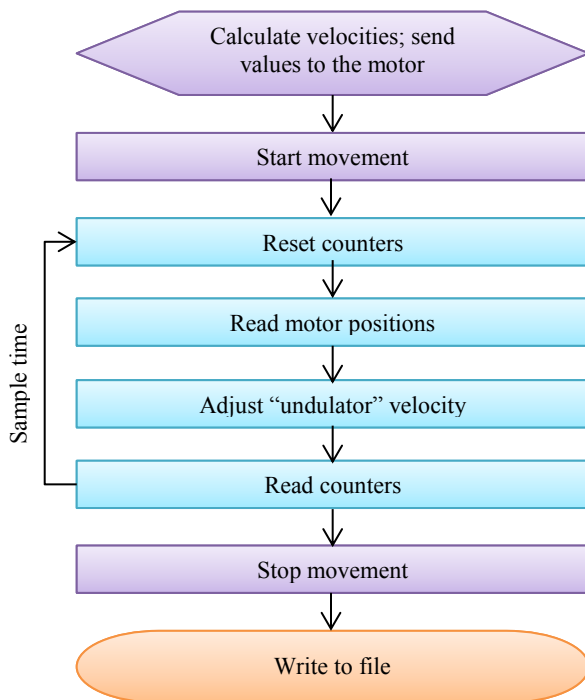


**Figure 1.** Flowchart of the control procedure

Bragg law  $E_{mono} = \hbar c / 2d \sin \Theta$ , where  $c$  denotes the speed of light in vacuum,  $\hbar$  - the Planck constant,  $d$  - spacing between lattice planes,  $\Theta$  - Bragg angle.

In the operational range of the undulator the shape of  $E_{und}(g)$  is almost linear while  $E_{mono}(\Theta)$  is cosecant and in case of the simultaneous linear movement of the motors along  $g$  and  $\Theta$  axes the misalignment between  $E_{und}$  and  $E_{mono}$  will reach 20 eV over the 1000 eV range. For the narrow spectral peak this energy difference can result in 25% variation of flux intensity and introduce unwanted variation in the spatial profile of the beam.

Therefore, the control routine includes the negative feedback loop which reads the positions of the motors defining the Bragg angle and undulator gap width from corresponding encoders, estimates the misalignment and regulates the motors movement. Due to limitations of the control system it was not possible to adjust the Bragg axis rotation speed once the movement was started, so the monochromator was set as the master device while the undulator operated in the slave mode making the gap width follow the rotation of the crystals. The desired energy range and total measurement time were set as initial parameters for the calculation of motor positions and movement velocities.

Resulting differences in the energy positions (synchronization precision) of undulator and monochromator did not exceed 2 eV over the range of 1000 eV, so that the beam was always matching the top of the undulator 3-rd harmonic peak.

The energy resolution was limited by the readout performance (sample time), that in turn is determined by the delay in communication between the beamline computer and Tango servers.

$$dE = t_{sample} \frac{E_{max} - E_{min}}{t_{total}}$$

Distribution of the readout time calculated from the timestamp is given at the figure 3, average sample time amounted  $\sim 45$ ms. Thus, for the 120s scan over a 1000 eV range one could estimate the energy step to be  $dE \sim 0.375$  eV and reaching up to 0.75 eV in certain points.

Our main goal was to synchronize the continuous Bragg axis movement with the undulator gap scan in order to match the same photon energy. The task is complicated by a nonlinear relation between the motor- and energy axes; for the undulator the photon energy is related to the gap width via the magnetic field:

$$E_{und} = \frac{9.5 E_e^2}{(1 + K^2/2)\lambda_u}$$

$$K = 0.0934 B_0 \lambda_u$$

$$B_0 = a_u \exp\left(b_u \left(\frac{g}{\lambda_u}\right) + c_u \left(\frac{g}{\lambda_u}\right)^2\right)$$

Here  $E_e$  is the particle energy in the storage ring in GeV,  $\lambda_u$  - undulator period in mm,  $K$  - deflection parameter,  $B_0$  - maximum magnetic field in T,  $g$  - full magnetic gap of the undulator in mm;  $a_u$ ,  $b_u$  and  $c_u$  - undulator-specific characteristic parameters [6]. Rotation of the Bragg axis of the monochromator is converted to the energy units according to the well-known

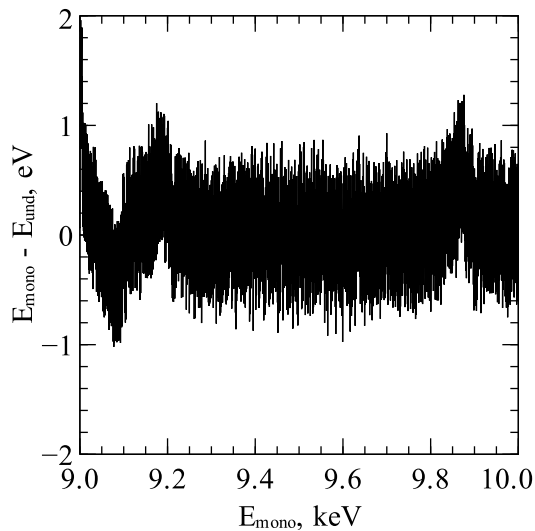


**Figure 2.** Energy misalignment in a 120s scan

experiment we collimated the beam to  $0.5 \times 0.5 \text{ mm}^2$  with the slits located 4 m upstream from the sample.

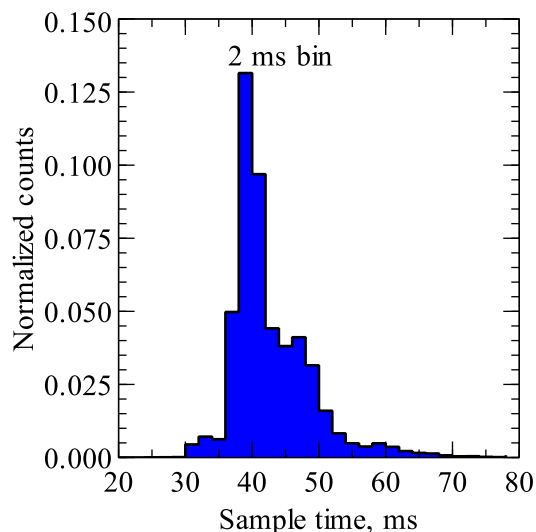


**Figure 3.** Distribution of the time-per-point in a 120s scan

In a 30s scan the XANES region is already distorted due to insufficient energy resolution, therefore, in order to have both long EXAFS and high quality XANES one needs a faster communication interface and faster electronics.

The other problem we address is the beam quality – both spatial and temporal. The beam is highly coherent in the vertical plane, so propagation through the entrance slit creates a pronounced Fresnel-like spatial pattern (figure 4). At the same time the long distance between the monochromator and the sample position converts small vibrations of the crystals into a perceptible beam movement across the sample. The combination of these factors drastically reduces the quality of the spectra of inhomogeneous samples (in contrast to the reference metal foils real powder samples are always inhomogeneous).

In order to minimize these effects in our

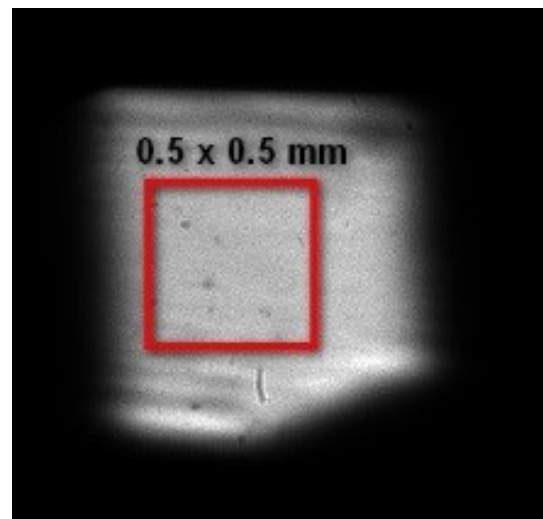


**Figure 4.** Beam profile at the sample

### 3. XAFS measurements

The sample was prepared according to standard procedures by pressing the grinded powder in a pellet with cellulose. X-ray absorption spectra previously measured at beamline C (DORIS) for this very sample were taken for comparison [7], identical EXAFS extraction parameters were used in both cases. The substance we used for the tests,  $\text{LuB}_{12}$ , allows measuring rather long EXAFS and features a sharp white line at the Lu  $L_{III}$  edge.

Custom built ionization chambers optimized for the high flux applications were used to measure the incident and transmitted beam intensity [8]. Both chambers were filled with nitrogen at optimal pressure and operated at high (2 kV) bias-voltage. The currents from the ionization chambers were amplified by Keithley 428 current amplifiers and digitized with 2 MHz VFC ADC [9].

The XANES spectrum and the  $k^2$  weighted EXAFS function are compared in figures 5 and 6 with the results from a conventional step scan (accumulation time increasing proportionally to  $k^2$  in EXAFS region). A slight deformation of the white line due to insufficient energy resolution is easily noticeable in the 30s scan.

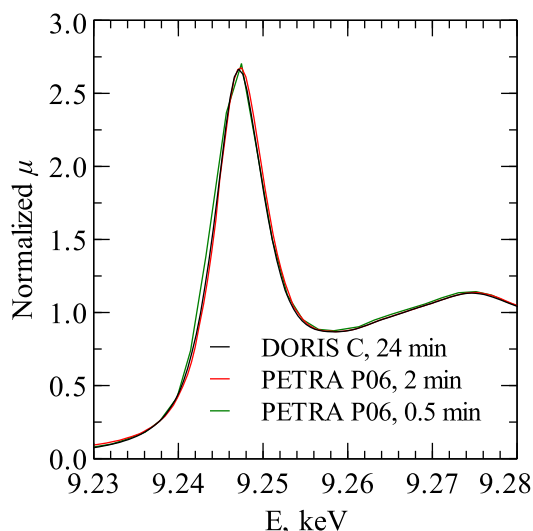


**Figure 5.** LuB<sub>12</sub> L<sub>III</sub>-Lu XANES

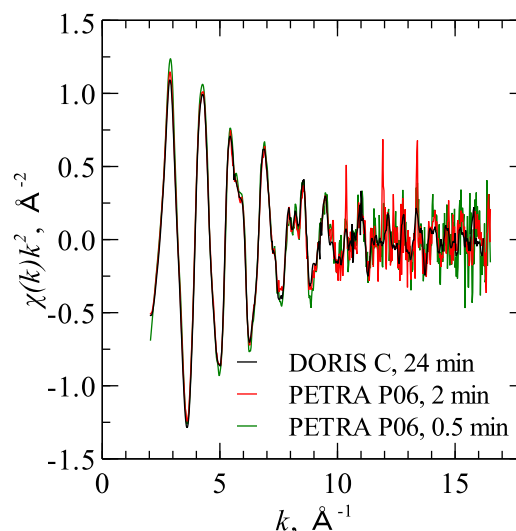


**Figure 6.** LuB<sub>12</sub> L<sub>III</sub>-Lu EXAFS function

High frequency oscillations in the high- $k$  region of EXAFS spectra do not distort the Fourier transform (not shown here) and allow accurate data reduction. Here the quality of the spectra is more likely limited by the inhomogeneity of the sample than by the insufficiency of the photon counts.

#### 4. Conclusion

We have proved the feasibility of fast EXAFS experiment in synchronous scan mode at the PETRA III undulator beamlines. We expect that this mode can be implemented at other beamlines built on the similar hardware and relying on TANGO as the control framework.

- [1] Rogalev A, Gotte V, Goulon J, Gauthier C, Chavanne J and Elleaume P 1998 *J. Synchrotron Rad* **5** 989
- [2] Oyanagi H, Ishii M, Lee C-H, Saini N, Kuwahara Yu, Saito A, Izumi Ya and Hashimoto H 1999 *J. Synchrotron Rad* **6** 155
- [3] Curtin M, Bhowmik A, Brown J, McMullin W, Metty P, Benson S V and Madey J M J 1990 *Nucl. Instrum. Methods Phys. Res. A* **296** 69
- [4] Boyanov B, Bunker G, Lee J M and Morrison T I 1994 *Nucl. Instrum. Methods Phys. Res. A* **339** 596
- [5] Schroer C, Boye P, Feldkamp J, Patommel J, Samberg D, Schropp A, Schwab A, Stephan S, Falkenberg G, Wellenreuther G and Reimers N 2010 *Nucl. Instrum. Methods Phys. Res. A* **616** 93
- [6] Kim K J 1989 *AIP Conf. Proc.* **184** 565
- [7] Menushenkov A P, Yaroslavtsev A A, Zaluzhnyy I A, Kuznetsov A V, Chernikov R V, Shitsevalova N Yu and Filippov V B 2013 *JETP Letters* **98** 165
- [8] Müller O, Stötzel J, Lützenkirchen-Hecht D and Frahm R 2013 *J. Phys.: Conf. Ser.* **425** 092010
- [9] Kracht Th and Zink H 2005 *HASYLAB Annual Report* **1** 119